Rheological investigations of water-soluble polysaccharides from the Tunisian brown seaweed *Cystoseira compressa*

Faiez Hentati[a,b], Guillaume Pierre[a], Alina Violeta Ursu[a], Christophe Vial[a], Cedric Delattre[a,c], Slim Abdelkafi[b], Philippe Michaud[a,*]

[a]Université Clermont Auvergne, CNRS, SIGMA Clermont, Institut Pascal, F-63000 Clermont-Ferrand, France.
[b]Unité de Biotechnologie des Algues, Biological Engineering Department, National School of Engineers of Sfax, University of Sfax, Sfax, Tunisia.
[c]Institut Universitaire de France (IUF), 1 rue Descartes 75005 Paris, France

*Corresponding author. Tel.: +33 (0) 4 73 40 74 25; Fax: +33 (0) 4 73 40 78 29
E-mail address: philippe.michaud@uca.fr (P.Michaud)

Abstract

Rheological characteristics of a sodium alginate and a fucoidan extracted from the brown seaweed *Cystoseira compressa* harvested from Kerkennah island (Sfax, Tunisia) were investigated. Steady-shear flow and dynamical viscoelasticity were evaluated to describe physicochemical properties of the GulA-rich alginate (ManA/GulA, M/G = 0.77) and highly-ramified fucoidan in semi-diluted media depending on polymer concentration, shear rate, temperature, added mono- (KCl and NaCl) and divalent ($CaCl_2$) salts. Alginate solutions exhibited shear-thinning behavior, with a temperature-dependent behavior highly correlated to the power-law model and the Arrhenius relationship. The results showed strong thixotropic and polyelectrolyte properties, influenced by addition of monovalent and divalent cations. The dynamic rheological characteristics showed a fluid-like viscoelastic behavior (tan δ > 1) whereas the critical overlap concentration C* and specific polymer constant k_s were respectively 11 $g.L^{-1}$ and 4.4 using Williamson model. Fucoidan solutions displayed a shear-thinning behavior with a low viscoelasticity character influenced by temperature and monovalent salts. The flow and viscoelastic characteristics of polysaccharides were described by the Ostwald model.

Keywords: Alginate, Fucoidan, *Cystoseira compressa*, Rheology.

1. Introduction

Polysaccharides are used in food industry and other as thickening, emulsifying, stabilizing and gelling agents (Ma, Lin, Chen, Zhao, & Zhang, 2014; Rioux, Turgeon, & Beaulieu, 2007). Among them, alginates from brown seaweeds are polyuronides composed of (1,4)-linked β-D-*p*mannuronic (M) and α-L-*p*guluronic acids (G) with $^4C_1$ and $^1C_4$ ring conformations respectively. These two uronic acids are organized as blocks of homopolymeric sequences (M- and G- blocks) separated by heteropolymeric ones (GM- or

MG- blocks). The distribution of these blocks and the M/G ratio depend on the seaweed species but also on the geographic origins and growth conditions (Fenoradosoa et al., 2010; Khajouei et al., 2018). Commercial alginates are extracted from a limited number of brown algae species including *Macrocystis pyrifera*, *Ascophyllum nodosum*, *Lessonia nigrescens*, *Ecklonia maxima*, *Laminaria* spp and *Durvillaea antarctica* well known for *(i)* their high-alginate content (up to 40% of the dry matter), *(ii)* the structural feature of their alginates and *(iii)* the G-blocks content of their alginates where selective alkaline earth metal multivalent cations such as Ca^{2+} take place by chelation. This chelation leads to the formation of strong alginate gels described by the popular "egg-box" model. It assumes that the G residues along the alginate chain have a 2_1 helical conformation and a pair of these chains is packed with calcium ions positioned between them (Plazinski, 2011). Alginates M/G > 1 are suitable to form elastic gels more than brittle ones (Hentati et al., 2018; Fenoradosoa et al., 2009; Braccini, Grasso, & Pérez, 1999; Grant, Morris, Rees, Smith, & Thom, 1973). Alginates are employed mainly in the food industry for their thickening and above all their gelifying characters (Sabra & Deckwer, 2005). The functional behaviors of several alginates have been studied in the last decades (Ma, Lin, Chen, Zhao, & Zhang, 2014; Sosa-Herrera, Lozano-Esquivel, de León-Ramírez, & Martínez-Padilla, 2012; Funami et al., 2009). Both M/G > 1 and M/G < 1 alginates in aqueous solutions revealed a pseudoplastic behavior at concentrations from 0.125 to 1.5 % (w/v) and temperatures ranging from 5 to 35 °C (Mancini, Moressi, & Sappino, 1996). For lower concentrations such as 0.1 % (w/v), solutions were described as Newtonian fluids for shear rate above 10 s^{-1}, highlighting the lack of intermolecular interactions due to electrostatic repulsion (Yang, Chen, & Fang, 2009). This Newtonian behavior can be also observed adding monovalent cations that act as counterions of anionic charges as reported by Rioux, Turgeon, and Beaulieu (2007).

Fucoidans from brown macroalgae are heterogeneous and ramified structures containing a linear backbone of α-L-fucopyranosyl residues (< 90%) linked in α-(1,3) and/or α-(1,4) branched at *O*-3 and *O*-4 positions by other neutral monosaccharides (*e.g.* Gal, Glc, Xyl, Man and uronic acids) (Berteau & Mulloy, 2003). Fucoidans have applications mainly in the field of bioactive compounds since their potential as technofunctional agent is limited (Sanjeewa et al., 2018; Palanisamy, Vinosha, Marudhupandi, Rajasekar, & Prabhu, 2017; Hifney, Fawzy, Abdel-Gawad, & Gomaa, 2016). Rioux, Turgeon, and Beaulieu (2007) studied the rheological Newtonian behavior of fucoidans isolated from three brown seaweeds and found that the variation observed in viscosity closely depended upon the molecular weight but also the content and positions of sulphate groups and uronic acids. Tako, Yoza, and Tohma (2000) also reported the viscoelasticity behavior of a fucoidan isolated from *Cladosiphon okamuranus,* positively influenced by salt, acid, and alkaline conditions.

Even if alginates and fucoidans have been abundantly studied and published these last years the interest of the academic community and industries for these old polysaccharides (especially alginates) is always substantial. Indeed, the world demand for texturing agents for conventional and new applications is in constant growth. For example, the sole alginate market share by food and pharmaceutic applications has increased by 20% during the last decade. It is mainly driven by high G type alginate even if high M type alginates have recently found applications. So even if the production capacity has expanded by 25%, mainly in China, the identification and exploitation of new alginate producers is of primary importance to support the world demand (Rein-Knudsen, Ale & Meyer, 2015). Considering commercial fucoidans from brown algae, they have been only used as ingredients in food supplements for at least two decades to support human health but also as topical cosmetic ingredients. Even if they are not yet used in any therapeutic application, the numerous biological activities linked to this sulphated polysaccharide could open new markets for it in a

93 next future. This observation justifies the research of new fucoidan sources. In this context,
94 *Cystoseira compressa* (Gerloff & Nizamuddin, 1975) which is a marine brown algae
95 (Phaeophyceae, Fucales) of Sargassaceae family, widely distributed along the Mediterranean
96 coasts was recently identified as a potential source of fucoidan and alginate (Hentati et al.,
97 2018). The extraction yields of alginates (21.65%) with significant M/G ratio (0.72) and
98 fucoidans (5.2%) were quite comparable or even superior to those of polysaccharides
99 commercially exploited from macroalgae. The correlation of their structures and their
100 physicochemical properties is then of primary importance to develop applications.
101 This paper deals with deep and comprehensive rheological investigations of solutions of
102 alginate (CCSA - 0.25-5.0 %, w/v) and fucoidan (CCF - 0.25-2.0 %, w/v) from *Cystoseira*
103 *compressa* to identify their putative applications as hydrocolloids.

104 ## 2. Materials and methods

105 ### 2.1. Algal material and chemicals

106 The brown seaweed *C. compressa* was harvested in February 2016 from Kerkennah Island
107 (Sfax, Tunisia), dried at 55 °C for 11 days, then ground into powder (0.3 mm mesh size) using
108 a mechanical blender (Moulinex). All used chemicals were purchased from Sigma-Aldrich
109 and of analytical grade.

110 ### 2.2. Extraction and purification of water-soluble polysaccharides

111 The polysaccharides were extracted according to the procedure described by Hentati et al.
112 (2018). Briefly, a succession of acid and alkaline extractions led to extract the matricial
113 polysaccharides from *C. compressa*. CCF (fucoidan) was extracted using an aqueous HCl (0.1
114 M) solution at 60 °C for 2 h according to the protocol proposed by Ermakova et al. (2013),
115 while CCSA (sodium alginate) was extracted by alkaline extraction with Na_2CO_3 (3.0 %, w/v)
116 using an adapted protocol from Davis, Ramirez, Mucci, and Larsen (2004). The two

polysaccharides were further purified according to the method reported by Hentati et al. (2018).

2.3. Rheological investigations

2.3.1. Sample preparation

Different concentrations of CCSA (0.25, 0.5, 0.75, 1.0, 1.5, 2.0, 3.0, 4.0 and 5.0 % (w/v)) and CCF (0.25, 0.5, 0.75, 1.0, 1.5 and 2.0 % (w/v)) solutions were prepared by solubilizing the dried powders in MilliQ water or in 0.1 and/or 0.5 M NaCl and/or KCl solutions after gentle stirring (400 rpm) until full dissolution (4 h at room temperature). The solutions were then stored at 4 °C for 48 h to obtain a full water-swelling polymer.

2.3.2. Rheological measurements

Rheological evaluations were performed using a rheometer AR-2000 (TA Instrument, Great Britain, Ltd) fitted with a 40 mm cone-plate geometry (54 microns gap) equipped with a Peltier heating system for accurate control. After loading, the samples were held for 15 min before measurements and then covered with a thin layer of hexadecane (Benaoun et al., 2017). The TA Instrument Rheology Advantage software (V5.7.0) was used to collect and analyze the rheological data. All rheological measurements in all tested conditions were performed in duplicate and the values of effectively overlapping traces were reported.

2.3.2.1. Steady-shear flow measurements

Steady-shear flow properties of CCSA (from 0.25 to 5.0 % (w/v)) and CCF (from 0.25 to 2.0 % (w/v)) solutions were investigated at 25 °C using the cone-plate geometry over the range of shear rate ($\dot{\gamma}$) from 0.001 to 1000 s^{-1}. The shear stress (τ) and apparent viscosity (η) were recorded as a function of shear rate ($\dot{\gamma}$) by applying the following model (Eq. 1):

$$\eta = \tau/\dot{\gamma} \qquad (1)$$

The Ostwald-de Waele model (Eq. 2) was used to fit the rheological data of CCSA, whereas CCF flow curves were analyzed using the power-law model (Eq. 2) and the Herschel-Bulkley model (Eq. 3).

$$\tau = k\,\dot{\gamma}^{n} \qquad (2)$$

$$\tau = \tau_0 + k\,\dot{\gamma}^{n} \qquad (3)$$

Where τ, τ_0, k and $\dot{\gamma}$ are respectively the shear stress (Pa), the yield stress (Pa), the consistency index (Pa.s^n) and the shear rate (s^{-1}), while n is the flow behavior index (dimensionless) which takes the values <1, 1 and >1 for pseudoplastic, Newtonian and plastic fluid behaviors, respectively.

2.3.2.2. Thixotropy and critical concentration determinations

The thixotropic characteristics of CCSA solutions (from 3.0 to 5.0 % (w/v)) were evaluated according to Ma et al. (2013) using hysteresis experiments which included three stages (upward curve (from 0.001 to 1000 s^{-1}), plateau curve (at 1000 s^{-1}) for 50 s and downward curve (from 1000 to 0.001 s^{-1})).

The critical overlap concentration (C*) of CCSA solutions (0.25 to 5.0 %, w/v), representing the limit between dilute (non-entangled system) and semi-dilute (entangled network) regimes in water at 25 °C, was expressed using the Williamson model (Eq. 4).

$$\eta = {}^{\eta_s}/_{1 + (K.\dot{\gamma})^{m}} \qquad (4)$$

Where η is the apparent viscosity (Pa.s), η_s is the zero shear viscosity (Pa.s), K is the time constant (s), $\dot{\gamma}$ is the shear rate (s^{-1}) and m is rate constant (dimensionless).

C* was calculated using the log-log plot of the specific viscosity (η_{sp}) *vs.* the concentration of polysaccharide.

2.3.2.3. Dynamic viscoelastic properties

Dynamic frequency sweep measurements were performed to determine and quantify the viscous and elastic responses of polysaccharidic solutions. The basis of these tests is the application of a sinusoidal strain of frequencies (rad/s or Hz) to the system and measuring its corresponding strain. For dynamic viscoelastic systems, the strain (%) and the stress (Pa) were out of phase. The oscillatory frequency sweeps for CCSA (3.0-5.0 %, w/v) and CCF (1.0-2.0 %, w/v) solutions at 25 °C in a constant strain of 20% (or in linear viscoelastic range) were carried out using the cone-plate geometry over the set of angular frequency (ω) ranging from 0.01 to 10 Hz (0.063-62.83 rad/s). The elastic modulus G' (storage modulus), viscous modulus G'' (loss modulus) and the loss tangent (tan $\delta = G''/G'$) (damping factor) as a function of angular frequency were continuously evaluated during the rheological analysis. The frequency dependence of G' and G'' was described by the power-law model (Eq. 5 and 6):

$$G' = k' (\omega)^{n'} \qquad (5)$$

$$G'' = k'' (\omega)^{n''} \qquad (6)$$

Where k' and k'' are constants, n' and n'' were the frequency exponents and can provide useful information concerning the viscoelastic features of food materials, ω is the angular frequency (rad/s or Hz).

The n' values were used as an indicator of the strength and nature of the gel; low n' values (near zero) reflects a covalent gel, whereas for $n' > 0$ (and close to 1) the system behaves as a viscous gel (physical gel) (Balaghi, Mohammadifar, Zargaraan, Gavlighi, & Mohammadi, 2011). The variation of k' and k'' values as well as n' and n'' ones is an indicator of the nature of the polymer behavior, $n'' > n'$ and $k' > k''$ reveal gel-like behavior while $n' >$ n" and $k'' > k'$ correspond to a viscous-like fluid.

2.3.2.4. Temperature-dependent behavior

The temperature influence (from 20 to 60 °C) on viscous properties of CCSA (from 3.0 to 5.0 % (w/v)) and CCF (from 1.0 to 2.0 % (w/v)) solutions were investigated by fitting the

aforementioned power-law model (Eq. 2) over the whole range of shear rate from 1.0 to 1000 s^{-1}. Additional viscoelastic experiments for CCSA (3.0-5.0 %, w/v) and CCF (1.0-2.0 %, w/v) solutions were conducted at different temperatures from 20 to 40 °C, and the range of angular frequency was set from 0.063 to 62.83 rad/s.

The temperature-dependent viscosity of CCSA aqueous solutions (3.0-5.0 % (w/v)) in the range of 20 to 45 °C at shear rate ranging from 1.0 to 1000 s^{-1} was evaluated according to the Arrhenius-Frenkel-Eyring model (Eq. 7):

$$\eta = A\, exp\left(Ea/RT\right) \qquad (7)$$

Where η is the apparent viscosity of fluid system (Pa.s), A is the proportionality constant (Pa.s), T is the absolute thermo-dynamical temperature (K), R is the universal gas constant ($kJ.mol^{-1}.K^{-1}$) and E_a is the flow activation energy, meaning the energy needed for the polymer units under applied shear ($kJ.mol^{-1}$).

The slope (E_a/R), the intercept (ln A) and the linear regression coefficient (R^2) were determined using the trend line of the plot of ln η versus $1/T$ (K^{-1}). The values of A and E_a were calculated using the exponential form of the intercept (ln A) and by multiplying the slope and gas constant (R) values, respectively.

2.3.2.5. Effect of salts on viscosity and viscoelastic properties

CCSA (3.0-5.0 %, w/v) and CCF (1.0-2.0 %, w/v) were dissolved in monovalent salts NaCl and KCl solutions at concentrations of (0.1-0.5 M). Indeed, the viscosities of alginates solutions depend as usually for polyuronides on the external monovalent cation concentration due to screening effect on electrostatic interactions and ionic strength. The NaCl contents of CCF and CCSA were previously evaluated at 1.88 and 1.28 % (w/w) (Hentati et al., 2018). The effect of shear rate (from 0.001 to 1000 s^{-1}) and angular frequency (of 0.063-62.83 rad/s) on viscosity as well as G' and G'' moduli were evaluated. 2.0 % (w/v) CCSA aqueous solutions (V = 5 mL) supplemented with $CaCl_2$ (from 4.58 to 5.66 mM) were investigated at

214 room temperature to determine the gelling point and the CCSA strength gel characteristics.
215 The shear and dynamic data were analyzed by fitting the power-law (Ostwald-de Waele)
216 model (Eqs. 2, 5 and 6).

217 3. Results and discussion

218 The structures of both CCF and CCSA fractions extracted from *C. compressa* were
219 described previously (Hentati et al. 2018). *C. compressa* sodium alginate (CCSA) was
220 composed of 56 % α-L-GulA (G) and 44 % β-D-ManA (M) (M/G = 0.72). The CCSA linear
221 backbone was constituted by 93 % of homoblocks (F_{GG} = 53 % and F_{MM} = 40 %) and 6 % of
222 heteroblocks (F_{MG} = 3 % and F_{GM} = 3 %) with a high distribution of homopolymeric blocks (η
223 = 0.13 < 1). The weight-average molar mass (M_w), number-average molar mass (M_n),
224 polydispersity index (Đ) and intrinsic viscosity ([η]) values were 1 × 10^5 g/mol, 6.5 × 10^4
225 g/mol, 1.5 and 400 mL/g, respectively (Hentati et al. 2018).

226 *C. compressa* fucoidan (CCF) was a highly-sulfated (14.7%) heterogalactofucan
227 composed of α-(1,3) and α-(1,4)-linked L-Fuc*p* as main backbone (1:0.26), highly-branched
228 (31.8 %) in *O*-3 and *O*-4 positions by terminal monosaccharides and side chains such as
229 terminal α-L-Fuc*p*, terminal β-D-Gal*p*, β-D-Gal*p*-(1→3)-α-L-Fuc*p* and β-D-Gal*p*-(1→4)-α-L-
230 Fuc*p*. The M_w, M_n, Đ and [η] for CCF were respectively 1.05 × 10^5 g/mol, 2.3 × 10^4 g/mol,
231 4.6 and 42 mL/g (Hentati et al. 2018).

232 3.1. Rheological features of CCSA

233 3.1.1. Steady-shear flow measurements of CCSA

234 The viscous characteristics at 25 °C of aqueous CCSA solutions at different
235 concentrations ranging from 0.25 to 5.0 % (w/v) were investigated using steady-shear flow
236 test over the shear rate ($\dot{\gamma}$) ranging from 0.001 to 1000 s^{-1} and the CCSA flow curves were
237 plotted over apparent viscosity (η) *vs.* shear rate ($\dot{\gamma}$) scale that covered six decades (Fig. 1A).

238 Depending on the CCSA concentration, different flow behaviors were observed due to the
239 various relations between viscosity and shear rate (Fig.1A).
240 The lower concentrations, below 2.0 % (w/v), exhibited a non-Newtonian shear-thinning
241 behavior at low shear rates ($\dot{\gamma} < \dot{\gamma}_c$) and a Newtonian behavior when the shear rate was
242 increased above a critical threshold ($\dot{\gamma} > \dot{\gamma}_c$), meaning that the CCSA flow behavior has
243 encountered more resistance at higher shear rates (Benchabane & Bekkour, 2008). The CCSA
244 concentration was inversely correlated with the size of the Newtonian plateau, indicating
245 intermolecular entanglements of CCSA in aqueous solution which tended to increase with
246 rising polymer concentration.
247 At concentrations above 2.0 % (w/v), the flow curves reported shear-thinning behavior with a
248 total absence of the Newtonian plateau region at the whole range of shear rates. These results
249 suggested that polymer chains adopted for these concentrations a more intertwined network in
250 the aqueous solution (Xiao, Tong, & Lim, 2012; Liu, Qian, Shu, & Tong, 2003). These
251 observations were in agreement with previous studies suggesting that the increasing of
252 sodium alginate or carboxymethyl cellulose (CMC) concentrations in aqueous solutions led to
253 transform their Newtonian behaviors into shear-thinning ones (Rioux, Turgeon, & Beaulieu,
254 2007; Ma, Lin, Chen, Zhao, & Zhang, 2014; Benchabane & Bekkour, 2008). Solutions of
255 alginate in water and at the same concentrations can sometimes have oppositional behaviors
256 i.e. Newtonian or non-Newtonian fluids, depending on their structures, molecular weights and
257 seaweed producers. In that respect, solutions of sodium alginate from *Nizimuddinia zanardini*
258 (1.0 to 5.0%, w/v) with a M/G ratio of 1.1 exhibited Newtonian or very low shear thinning
259 behaviors whereas those of Ma et al. (2014) composed of a commercial G-rich sodium
260 alginate had a shear thinning one at identical concentrations. However, at the concentrations
261 used in food industry (above 2% (w/v)) alginates are Non-Newtonian pseudoplastic fluids.

The data and the shear parameters for different CCSA aqueous solutions (2.0-5.0 % (w/v)) were evaluated by fitting the Ostwald-de Waele model and were presented in Table 1. The solutions of 2.0-5.0 % (w/v) CCSA confirmed the property of a shear-thinning fluid possessing values of flow behavior index n less than 1. The rise in polymer concentration caused an increase in the coefficient of consistency (k) and a decrease in the n values. Regarding the coefficients of determination (R^2), the CCSA solutions (3.0, 4.0 and 5.0 %, w/v) flow curves had important linear correlations to the Ostwald-de Waele model (generally $R^2 > 0.99$), showing that the CCSA rheological behavior was suitably described by the power-law model for aqueous solutions above 2.0 % (w/v) over the shear rate scale ranging from 0.001 to 1000 s^{-1} at 25 °C. These results were in accordance with those of literature, (Ma, Lin, Chen, Zhao, & Zhang, 2014; Cevoli, Balestra, Ragni, & Fabbri, 2013; Clementi, Mancicni, & Moresi, 1998) for alginates solutions having rheological behaviors well described by the power-law model for concentrations below 1.5 % (w/v). On the contrary, Ma, Lin, Chen, Zhao, and Zhang (2014), Cevoli, Balestra, Ragni, and Fabbri (2013) and Xiao, Tong, and Lim (2012) showed a weak adjustment achieved by the power-law model, respectively for alginate concentrations, ranging from 1.5 to 3.0 % (w/v) over the shear rate between 0.01 and 1000 s^{-1}, from 2.0 to 2.5 % (w/v) over the shear rate of 0 to 300 s^{-1} and finally from 4.0 % (w/v) over the shear rate from 0.1 to 100 s^{-1}.

3.1.2. Effect of temperature on the viscosity of CCSA aqueous solutions

Supplementary shear tests for aqueous CCSA solutions of 5.0 % (w/v) were performed at temperatures ranging from 20 to 60 °C over a wide range of shear rates (from 1 to 1000 s^{-1}) (Fig. 2A). The apparent viscosity dropped with the increase of temperature from 20 to 60 °C and a pseudoplastic behavior was observed. The weakening of η values can be linked to the thermal expansion, phenomenon rising intermolecular distances by minimizing the interactions and entanglements between CCSA blocks (Benaoun et al., 2017).

The rise in temperature increased the n and R^2 values (> 0.99), but decreased the k magnitudes (see Supplementary data), indicating that heat treatment slowed the CCSA pseudoplastic properties but still retaining the values of n less than 1 and the ability of power-law flow model to describe the temperature-dependent behavior in the range 20-60 °C. These results were in accordance with those previously reported for alginate and other polysaccharides such as heteroxylan, xanthan gum, or sodium carboxymethyl cellulose (Benaoun et al., 2017; Ma, Lin, Chen, Zhao, & Zhang, 2014; Kechinski, Schumacher, Marczak, Tessaro, & Cardozo, 2011; Yang & Zhu, 2007). This great dependence to temperature could be attributed to the conformational change of the CCSA macromolecules or to a molecular equilibrium transition to another one less stable accompanied by the thermal expansion phenomenon (De Paula & Rodrigues, 1995).

The Arrhenius-Frenkel-Eyring form (Keleşoğlu, Pettersen, & Sjöblom, 2012) was applied to verify these hypotheses. As shown in Fig. 2B, high values of E_a implied that CCSA solutions were more sensitive to the temperature. The data illustrated in Table 2 showed that the polymer viscosity was decreased by rising temperature and the E_a values tended to drop with the rise of shear rate, suggesting that the CCSA aqueous solutions flowed more readily under shearing (Razmkhah, Razavi, & Mohammadifar, 2017). For all CCSA tested solutions (3.0-5.0 % w/v), the perfectly linear shape (R^2 > 0.99) of the flow curves obtained by fitting the Arrhenius equation (Vinogradov & Melkin, 1980) confirmed a complete absence of both conformational changes and chain destruction of CCSA blocks under the effect of rising temperature (De Paula, Santana, & Rodrigues, 2001). These results suggested that the rise of temperature increased the energy dissipation motions of macromolecules, which resulted in a breakdown of the weak energy bonds and the decrease of the intermolecular interactions and consequently of flow activation energy (E_a) (Chen & Chen, 2001). This temperature-

dependent result for CCSA solutions was a kind of substantial non-Newtonian fluid characteristics.

3.1.3. Effect of monovalent salts on the CCSA viscosity

The effect of monovalent cations Na^+ and K^+ (0.1-0.5 M) on steady-shear flow properties of CCSA solutions (3.0-5.0 %, w/v) was investigated using 0.001-1000 s^{-1} shear rate range (Fig. 1B).

In presence of 0.5 M monovalent cation, the CCSA (3.0-5.0 %, w/v) exhibited a pseudoplastic behavior showing that alginate chains adopted a more entangled network wherein the acidic blocks (especially GG blocks) intertwined with each other by increasing the number of junction zones and thus reinforcing a more viscous network (Xiao, Tong, & Lim, 2012). The rise in apparent viscosity of alginate in NaCl solution seemed more important than for K^+, presenting then a significant ionic selectivity explained by the Hofmeister series ($Na^+ > K^+$) (Carr, Munro, & Campanella, 2002). Na^+ ions confer to CCSA a stiffer inner structure due to the significant increase in entanglements and inter-block interactions that tend to improve the dimensions of the polymer coils, whereas, these phenomena were reduced in the presence of monovalent ions K^+. This result was similar to those obtained by Draget et al. (2006) or Ma et al. (2014) who had observed a significant increasing of alginate solutions viscosities after NaCl addition. This phenomenon was more pronounced for alginates with high G contents.

The ionic strength-dependent behavior was evaluated adjusting the power-law model (Table 3). Data confirmed that the monovalent cations addition caused the increase of the pseudoplastic character of CCSA solutions by amplifying the consistency index k and decreasing the flow behavior index n. Regarding the n and k values, the ionic selectivity occurrence was confirmed (Seale, Morris, & Rees, 1982). This result and the structural features of CCSA with a F_{GG} = 53 % and a η parameter below 1 (η = 0.13) are in agreement

with the results reached by Grant, Morris, Rees, Smith, and Thom (1973) who revealed conformational changes of alginates due to increased electrostatic interactions between GG blocks. For coefficients R^2, the Ostwald-de Waele model was less suitable ($0.96 < R^2 < 0.99$) to describe flow curves for CCSA in salts media.

3.1.4. Dynamic viscoelastic properties of CCSA

The dynamic mode sweep analyses were performed on CCSA solutions (3.0-5.0 %, w/v) at 25 °C in MilliQ water (Fig. 3A) and in salt solutions (0.5 M NaCl and 0.5 M KCl) (Fig. 3B).

As shown in Fig. 3A, the elastic modulus (G') and the viscous modulus (G'') increased with increasing concentrations and angular frequencies (ω) at 25 °C. Note that the same moduli decreased with the increase of temperature ranging from 20 to 40 °C (data not shown). The CCSA samples exhibited a typical viscous liquid-like behavior as the G'' values were greater than the G' values throughout the frequency range 0.063-62.83 rad/s. These results are in accordance with those obtained with a commercial sodium alginate (2.5 %, w/v) (Ma, Lin, Chen, Zhao, & Zhang, 2014). In this case the two moduli tended to approach each other at high frequencies. Another sodium alginate solution at 2.0 % (w/v) showed also larger values for G" than for G' but higher differences between G' and G" (Belalia & Djelali, 2014). The dynamic mechanical loss tangent ($\tan \delta = G''/G'$) is a characteristic parameter for the assessment of the viscoelastic behavior (Razmkhah, Razavi, & Mohammadifar, 2017). The $\tan \delta < 1$ designates an elastic behavior, whereas $\tan \delta > 1$ denotes a viscous one. The values of $\tan \delta$ were greater than 1 and confirmed the presence of fluid-like viscous behavior for all CCSA solutions in water. Both moduli tended to approach each other, revealing that the $\tan \delta$ values dropped with increasing frequencies and the polymer energy was dissipated by a viscous flow, indicating a great CCSA viscoelastic behavior ($0 < \delta < \pi/2$). The deformation-dependent viscoelastic behavior of CCSA implied that at weak deformations, the polymer

chains had enough time to relax to a more stable molecular state by gliding the overlap point of the CCSA chains (Ma, Lin, Chen, Zhao, & Zhang, 2014). The opposite case was observed at higher sinusoidal deformations and was explained by the great temporary power of energy storage by the GG blocks constituting the CCSA chain (Doi & Takimoto, 2003).

The power-law model (section 2.3.2.3) was also used to describe the dependency relationship between angular frequency (ω) variation and viscoelasticity moduli (G' and G''). The high values of n' and n'' (Table 4) confirmed the CCSA viscous-like behavior (Balaghi, Mohammadifar, Zargaraan, Gavlighi, & Mohammadi, 2011) and indicated that CCSA solutions (3.0-5.0%, w/v) displayed great frequency dependency. The n' magnitudes were greater than n'' and k' values were lower than those of k'', clearly indicating that G' increased at a higher rate than G'' (Razavi, Cui, & Ding, 2016). The n' and n'' values dropped with rising concentrations from 3.0 to 5.0 % (w/v), reflecting the drop in frequency sensitivity, while the increase in the k' and k'' suggested the formation of highly viscous networks by increasing the entanglement points and intermolecular junction zones (Razmkhah, Razavi, & Mohammadifar, 2017). According to the important regression coefficient values ($R'^2 > 0.99$ and $R''^2 > 0.99$), the dynamical oscillatory curves of the aqueous CCSA solutions were perfectly described by the power-law model.

Additional dynamic oscillatory experiments at 25 °C for CCSA solutions (3.0 and 5.0% (w/v)) in NaCl and KCl 0.5 M solutions were conducted at the range of angular frequency from 0.063 to 62.83 rad/s (Fig. 3B). G' and G'' values increased with the addition of monovalent cations in the solutions, confirming again the strong polyelectrolyte character of CCSA.

Depending on CCSA concentration, angular frequencies and nature of monovalent cation, different viscoelastic behaviors were observed. Considering solutions of CCSA with concentration below 5 % (w/v), G'' values were greater than G' ones and tan $\delta > 1$

demonstrating a typical viscous behavior. The 5.0 % (w/v) CCSA solution in 0.5 M NaCl gave an elastic response ($G' > G''$) at low deformations ($\omega \leq$ 1rad/s) typical of weak-gel structure ($0 < \tan \delta < 1$). At the same concentration, CCSA was not able to form a gel in the presence of KCl ($\tan \delta > 1$, $G'' > G'$), confirming the high selectivity for Na^+ ions relative to K^+ ones (Fig. 3B).

The values of n' and n'' obtained with the power-law model (Table 4) decreased with monovalent cation concentrations, whereas those of k' and k'' increased leading to the conclusion that the frequency sensitivity dropped and the CCSA viscous network got stronger in the presence of monovalent cations. The lowest CCSA concentration (3.0 %, w/v) in 0.5 M KCl displayed n' values (0.91) greater than that of n'' (0.83), whereas at 5.0 % (w/v) in the same KCl solution, the n'' value (0.70) became higher than n' one (0.61). This result indicated that G'' increased at a higher rate than G' with increasing frequency (k'' values remained higher than those of k').

In 0.5 M NaCl, the 3.0 % (w/v) CCSA solution exhibited a viscoelastic behavior with n'' and k'' being higher than n' and k'. However, k' value was larger than k'' one for 5.0 % (w/v) CCSA solution reflecting a typical weak gel-like behavior and confirming the ionic selectivity for Na^+.

These results confirmed the observations of Fig. 3B and indicated that the complexity degree of the junction regions between CCSA (5.0 %, w/v) chains was increased at low angular frequencies and the increasing angular frequencies ($\omega >$ 1 rad/s) disrupted gel conformational equilibrium by favoring a viscous behavior qualified by $G'' > G'$ values as reported by other authors (Ma, Lin, Chen, Zhao, & Zhang, 2014; Simas-Tosin et al., 2010).

3.1.5. Effect of divalent cations on CCSA solutions

Steady-shear flow and dynamic oscillatory measurements were applied to 2.0 % (w/v) CCSA solutions in 4.58-5.66 mM $CaCl_2$ to determine the liquid-gel transition (gelling point)

411 of CCSA. The addition of $CaCl_2$ significantly increased the CCSA (2.0%, w/v) flow viscosity
412 for all shear rates (0.001-1000 s^{-1}) (Fig. 4A). All CCSA solutions supplemented with calcium
413 exhibited a non-Newtonian shear-thinning behavior. This result is in accordance with those
414 presented by Sosa-Herrera, Lozano-Esquivel, de León-Ramírez, and Martínez-Padilla (2012)
415 for sodium alginate gum from brown seaweed. The increase in η values was attributed to the
416 formation of a networks crosslinked by transverse bonds between guluronic residues (GG
417 blocks) in presence of Ca^{2+} ions (Liu, Qian, Shu, & Tong, 2003).

418 Based on the Ostwald-de Waele model, the addition of $CaCl_2$ dropped the n values from
419 0.77 to 0.22 and greatly increased the k ones (from 0.14 to 14.59) showing an improvement of
420 the pseudoplastic character of CCSA gels (see Supplementary data). As shown in Fig. 4B, the
421 values of G' and G'' moduli increased with $CaCl_2$ concentrations from 4.58 to 5.66 mM. The
422 G' was higher than G'' ($0.1 < \tan \delta < 1$) indicating that CCSA exhibited a typical weak gel-like
423 behavior with a weak dependence of both moduli on frequency (Clark & Ross-Murphy,
424 1987).

425 These results were again confirmed by the decrease of n' (from 1.46 to 0.10), n'' (of 0.99
426 to 0.25) values and by the increase of k' (0.001-45.71) and k'' (0.08-9.59) (Table 5).
427 In presence of Ca^{2+} ions, the n'' values (0.25-0.35) were larger than n' ones (0.10-0.14)
428 meaning that G'' increased with higher rates than G'. The k' magnitudes were greater than
429 those of k'', confirming the weak-gel behavior of CCSA. According to the values of R'^2 and
430 R''^2, the power-law model was not adapted to describe the viscoelastic behavior of CCSA in
431 calcium solutions.
432 The addition of $CaCl_2$ solution at a 4.58 mM for 2.0 % (w/v) CCSA solution revealed the
433 maximum viscosity reached without forming a gel. At the Ca^{2+} concentration of 4.94 mM, the
434 gelling transition point was visually observed as the fluid behavior of CCSA was replaced by
435 a weak-gel one undisturbed by mechanical agitation. These observations were confirmed by

436 the variation of tan δ values as a function of angular frequencies and $CaCl_2$ concentrations
437 (see Supplementary data). The tan δ values tended to decrease (near to 0.1 for strong gel) with
438 the rise of $CaCl_2$ concentration and the decrease of angular frequencies. These results
439 indicated that the junction zones between the CCSA blocks (especially GG blocks) increased,
440 promoting the dimerization and aggregation of alginate chains according to the "egg box"
441 model (Grant, Morris, Rees, Smith, & Thom, 1973; Simas-Tosin et al., 2010). This ability of
442 alginates to form gels with calcium and the strength of these gels depends strongly on their G
443 contents but also on their molecular weights (Fernandez & Norton, 2014). Logically, high
444 Mw alginates have faster gel formation kinetics than those of fluid gels produced with low
445 Mw alginates.

446 **3.1.6. Thixotropy**

447 Many hydrocolloids solutions are well known for their time-dependent characteristics,
448 which mean that the apparent viscosity varies with shearing time (Benchabane & Bekkour,
449 2008). In contrast to the rheopexy which is a rare phenomenon, thixotropy is a current
450 property for non-Newtonian alginate solutions where the polymer viscosity decreased with
451 shearing time action (Ma, Lin, Chen, Zhao, & Zhang, 2014).
452 The hysteresis loop method (Razmkhah, Razavi, & Mohammadifar, 2017) was used to
453 characterize the viscosity-time relationship of CCSA and the gap between the up and down
454 curves.
455 As shown in Fig. 5A, the hysteresis loops of CCSA aqueous solutions at each concentration
456 revealed thixotropic characteristics which tended to increase slowly with the rise of alginate
457 concentration from 3.0 to 5.0 % (w/v). Consequently, the time dependence was stronger. High
458 negative values of hysteresis loop implied that the damage of CCSA macromolecules was
459 stronger. These results agreed with the literature (Ma, Lin, Chen, Zhao, & Zhang, 2014;
460 Benchabane & Bekkour, 2008), where the thixotropic behavior was confirmed for sodium

alginate and CMC solutions at different tested concentrations. These papers revealed that the decrease in viscosity with shearing time was mainly due to the shear-thinning behavior, the disentanglement-entanglement processes and also to the alignments disturbances of the polymer chains.

3.1.7. Critical overlap concentration (C*) determination

The critical overlap concentration (C*) represents the limit between two areas, dilute and semi-dilute regimes. It was deduced from the log-log plot of specific viscosity (η_{sp}) *vs.* polysaccharide concentration (Fig. 5B). The η_{sp} increased with increasing CCSA concentrations and the slope break indicated the experimental C* (Chouana et al., 2017). The C* of CCSA solutions without salts at 25 °C was 11 g.L^{-1} and the slopes of the linear segments below and above the C* values were, respectively, about 1.3 and 4.9.

The C* is an inverse function of the intrinsic viscosity as expressed by Eq. 7:

$$C^* = k_s/[\eta] \qquad (7)$$

Where the constant k_s (values between 0.77 and 4) is specific for each type of polysaccharides (Chouana et al., 2017; Lapasin & Pricl, 1999; Norton et al., 1984; Doublier & Launay, 1981). For CCSA, the k_s value was calculated at 4.4. These results were consistent with the literature concerning alginate solutions (random coil polysaccharide) extracted from brown seaweeds (Morris, Rees, & Thom, 1980) when the C* value is around 4/[η] for a zero-shear specific viscosity (η_{sp}) value near to 10.

3.2. Rheological properties of CCF

The viscous and dynamic properties for aqueous CCF solutions from 0.25 to 2.0 % (w/v) concentrations were also conducted in this study. Fig. 6A gave the plot of log-log scale in terms of viscosity as a function of shear rate from 0.01 to 1000 s^{-1}. For all tested concentrations, CCF solutions exhibited non-Newtonian shear-thinning behavior at low shear rate, below the critical shear rate ($\dot{\gamma}_c$) (1-10) s^{-1}, while Newtonian behavior was observed at

higher shear rate above this critical threshold ($\dot{\gamma} > \dot{\gamma}_c$). The $\dot{\gamma}_c$ values increased from 1 to 20 s^{-1} with the polysaccharide concentration (0.25-2.0 % (w/v)). The decrease of the apparent viscosity of CCF was explained by the disruption of its molecular entanglements when the shear rate increased. The Newtonian plateau region well observed for lower concentrations tended to disappear when they were greater (0.25 to 2.0 % (w/v)) (Calero, Muñoz, Ramírez, & Guerrero, 2010; Tako, 2003).

These observations were in accordance with previous rheological investigations on fucoidans extracted from *Fucus vesiculosis*, *Ascophyllum nodosum* and *Saccharina longicruris* (Rioux, Turgeon, & Beaulieu, 2007). These results differed from those of fucoidan extracted from sea cucumber (*Thelenota ananas*) which presented shear-thinning behavior when polysaccharide concentration and shear rate ranged from 0.1 to 17.5 $g.L^{-1}$ and from 0.1 to 1000 s^{-1} (Xu, Xue, & Chang, 2017). The flow properties of fucoidan isolated from *Cladosiphon okamuranus* exhibited shear-thinning behavior at weak concentrations (1.0 and 1.5 % (w/v)) and shear-thickening behavior at high ones above 2.0 % (w/v) (Tako, 2003). Moreover, Yu et al. (2015) reported pseudoplastic behavior of fucoidan solutions from *Apostichopus japonicus* at low shear rate (1-100 s^{-1}) while a shear-thickening one was observed for shear rates above 100 s^{-1}. Regarding the literature, this broad variability recorded in rheological behaviors depends on the molecular weight, the proportion and position of sulphates groups and uronic acids, but also probably on the branching structures (Katayama, Nishio, Iseya, Kishimura, & Saeki, 2009; Tako, 2003).

The shear rheological data of CCF solutions were analyzed by fitting the Herschel-Bulkley (data not shown) and the Ostwald-de Waele models as illustrated in Table 1. The *n* values were closed to 1, meaning that CCF exhibited a very low pseudoplastic behavior at concentrations from 0.25 to 2.0 % (w/v). The rise in CCF concentration caused a decrease in

510 the n values (from 1.09 to 0.59) and an increase in k values (from 0.004 to 0.077) as reported
511 by Rioux, Turgeon, & Beaulieu (2007).
512 Fig. 6C showed that the shear viscosities of the 2.0 % (w/v) CCF solution decreased with the
513 rise of the temperatures from 20 to 60 °C over all shear rates from 0.1 to 1000 s^{-1}.
514 The salt-dependent behavior of CCF was also evaluated at 25 °C using NaCl and KCl at 0.1
515 and 0.5 M (Fig. 6B). The addition of salts dropped the apparent viscosity of a 2.0 % (w/v)
516 CCF solution and the shear-thinning behavior was retained for shear rates below the critical
517 one and a weak ionic selectivity for Na^+ monovalent ion was also detected. The values of n
518 increased while a decrease in k values was recorded (Table 3).
519 These observations were in accordance with previous studies carried out on fucoidans
520 extracted from *Apostichopus japonicas* and *Accaudina molpadioides* (Yu et al., 2015).
521 According to Simas-Tosin et al. (2010), the drop of viscosity can be explained by the decrease
522 of intermolecular electrostatic repulsions between CCF chains and by the reduction of
523 junction zones between CCF molecules in the presence of monovalent salts leading more
524 compact conformation of CCF macromolecules.
525 The viscoelastic characteristics of CCF solutions (1.0 and 2.0 %, w/v) at 25 °C were evaluated
526 using the dynamical oscillatory frequency sweep tests (Fig. 7A). CCF solutions presented
527 typical viscous-like behavior since G'' was higher than G'. Moreover, the gap between these
528 both moduli slightly decreased at high frequencies, highlighting low viscoelastic properties,
529 which involved that most of the energy was dissipated by viscous flow (Ma, Lin, Chen, Zhao,
530 & Zhang, 2014). The addition of monovalent salts slightly decreased the G' and G'' values, G''
531 values remaining larger than G' ones and the tan δ decreasing at high frequencies (Fig. 7A).
532 The addition of salts decreased the values of k' and k'' (but $k'' > k'$) and increased those of n'
533 and n'' ($n' > n''$) (Table 4) confirming again that CCF exhibited viscous-like behavior and the
534 viscoelastic properties tended to decrease with adding monovalent salts (Simas-Tosin et al.,

535 2010). The ion-dependent behavior was due to the highly-branched form and the weak
536 electrolyte nature of CCF, which revealed that addition of monovalent salts led to structural
537 changes that affected rheological behavior by breaking intermolecular interactions,
538 entanglement points, junction zones and then decreasing repulsion phenomenon, causing thus
539 more compact form of CCF in salts (Oliveira, Silva, De Paula, Feitosa, & Paula, 2001).

540 **4. Conclusion**

541 The main goals of this study were the characterization of rheological properties of an alginate
542 (CCSA) and a fucoidan (CCF) isolated from the Tunisian brown seaweed *C. compressa*.
543 CCSA solutions (0.25-5.0 % (w/v)) exhibited a shear-thinning behavior with the presence of a
544 Newtonian plateau for the lowest concentrations (below 2.0% (w/v)) at high shear rates. The
545 temperature-dependent behavior of 3.0-5.0 % (w/v) CCSA solutions had higher correlation to
546 the power-law model and the Arrhenius-Frenkel-Eyring relationship. CCSA solutions at 5.0
547 % (w/v) in 0.5 M NaCl had weak-gel structures and a gelling point was identified for 2.0%
548 (w/v) solution at 4.94 mM of $CaCl_2$. The CCSA solutions presented a thixotropic behavior
549 and C* and k_s were respectively of 11 $g.L^{-1}$ and 4.4. The dynamical viscoelastic properties
550 showed a fluid-like viscoelastic behavior ($G'' > G'$) with a great viscoelastic character.
551 CCF solutions (0.25-2.0 % (w/v)) showed pseudoplastic behavior at low shear rate and
552 Newtonian plateau above a critical shear rate. A fluid-like viscoelastic behavior was observed
553 and both moduli (G'' and G') increased with the increase of angular frequency and
554 concentrations but decreased with the rise of temperatures and salts concentrations, showing
555 the weak polyelectrolyte character of this polysaccharide.
556

557 **Acknowledgements**

558 This work has been sponsored by the Tunisian Ministry of higher education and scientific
559 research and Campus France (714305B) (Eiffel scholarship program of excellence, 895151J).

560 **References**

561 Balaghi, S., Mohammadifar, M. A., Zargaraan, A., Gavlighi, H. A., & Mohammadi,
562 M. (2011). Compositional analysis and rheological characterization of gum tragacanth
563 exudates from six species of Iranian *Astragalus*. *Food Hydrocolloids*, *25*(7), 1775–1784.

564 Belalia, F., & Djelali, N. E. (2014). Rheological properties of sodium alginate
565 solutions. *Revue Roumaine de Chimie. 59*, 135–145.

566 Benaoun, F., Delattre, C., Boual, Z., Ursu, A. V., Vial, C., Gardarin., et al. (2017).
567 Structural characterization and rheological behavior of a heteroxylan extracted from *Plantago*
568 *notata* Lagasca (Plantaginaceae) seeds. *Carbohydrate polymers*, *175*, 96–104.

569 Benchabane, A., & Bekkour, K. (2008). Rheological properties of carboxymethyl
570 cellulose (CMC) solutions. *Colloid and Polymer Science*, *286*(10), 1173.

571 Berteau, O., & Mulloy, B. (2003). Sulfated fucans, fresh perspectives: structures,
572 functions, and biological properties of sulfated fucans and an overview of enzymes active
573 toward this class of polysaccharide. *Glycobiology*, *13*(6), 29R–40R.

574 Braccini, I., Grasso, R. P., & Pérez, S. (1999). Conformational and configurational
575 features of acidic polysaccharides and their interactions with calcium ions: a molecular
576 modeling investigation. *Carbohydrate Research*, *317*(1–4), 119–130.

577 Calero, N., Muñoz, J., Ramírez, P., & Guerrero, A. (2010). Flow behaviour, linear
578 viscoelasticity and surface properties of chitosan aqueous solutions. *Food*
579 *Hydrocolloids*, *24*(6–7), 659–666.

580 Carr, A. J., Munro, P. A., & Campanella, O. H. (2002). Effect of added monovalent or
581 divalent cations on the rheology of sodium caseinate solutions. *International dairy*
582 *journal*, *12*(6), 487–492.

583 Cevoli, C., Balestra, F., Ragni, L., & Fabbri, A. (2013). Rheological characterization
584 of selected food hydrocolloids by traditional and simplified techniques. *Food hydrocolloids*,

585 *33*(1), 142–150.

586 Chen, R. H., & Chen, W. Y. (2001). Rheological properties of the water-soluble
587 mucilage of a green laver, *Monostroma nitidium*. *Journal of Applied phycology*, *13*(6), 481–
588 488.

589 Chouana, T., Pierre, G., Vial, C., Gardarin, C., Wadouachi, A., Cailleu, D., et al.
590 (2017). Structural characterization and rheological properties of a galactomannan from
591 *Astragalus gombo* Bunge seeds harvested in Algerian Sahara. *Carbohydrate polymers*, *175*,
592 387–394.

593 Clark, A. H., & Ross-Murphy, S. B. (1987). Structural and mechanical properties of
594 biopolymer gels. In *Biopolymers* (pp. 57–192). Springer, Berlin, Heidelberg.

595 Clementi, F., Mancini, M., & Moresi, M. (1998). Rheology of alginate from
596 *Azotobacter vinelandii* in aqueous dispersions. *Journal of food engineering*, *36*(1), 51–62.

597 Davis, T. A., Ramirez, M., Mucci, A., & Larsen, B. (2004). Extraction, isolation and
598 cadmium binding of alginate from *Sargassum spp*. Journal of Applied Phycology, 16, 275–
599 284.

600 De Paula, R. C. M., & Rodrigues, J. F. (1995). Composition and rheological properties
601 of cashew tree gum, the exudate polysaccharide from *Anacardiumo ccidentale*
602 L. *Carbohydrate Polymers*, *26*(3), 177–181.

603 De Paula, R. C. M., Santana, S. A., & Rodrigues, J. F. (2001). Composition and
604 rheological properties of *Albizia lebbeck* gum exudate. *Carbohydrate polymers*, *44*(2), 133–
605 139.

606 Doi, M., & Takimoto, J. I. (2003). Molecular modelling of entanglement.
607 Philosophical Transactions. *Series A: Mathematical, Physical and Engineering Sciences*, *361*,
608 641–652.

609 Doublier, J. L., & Launay, B. (1981). Rheology of galactomannan solutions:
610 comparative study of guar gum and locust bean gum. *Journal of Texture Studies*, *12*(2), 151–
611 172.
612 Ermakova, S., Men'shova, R., Vishchuk, O., Kim, S. M., Um, B. H., Isakov, V., &
613 Zvyagintseva, T. (2013). Water-soluble polysaccharides from the brown alga *Eisenia bicyclis*:
614 Structural characteristics and antitumor activity. *Algal Research*, *2*(1), 51–58.
615 Fenoradosoa T.A., Ali G., Delattre C., Laroche C., Petit E., Wadouachi A., Michaud
616 P. (2010). Extraction and characterization of an alginate from the brown seaweed *Sargassum*
617 *turbinarioides* Grunow. *Journal of Applied Phycology* 22(2): 131-137.
618 Fernandez Farres, I., & Norton, I.T. (2014). Formation kinetics and rheology of
619 alginate fluid gels produced by in-situ calcium release. *Food Hydrocolloids*, *40*, 76-84.
620 Funami, T., Fang, Y., Noda, S., Ishihara, S.,Nakauma, M., Draget, K. I., et al. (2009).
621 Rheological properties of sodium alginate in an aqueous system during gelation in relation to
622 supermolecular structures and Ca^{2+} binding. *Food Hydrocolloids*, *23*(7), 1746–1755.
623 Gerloff, J., & Nizamuddin, M. (1975). Bemerkungen zur Nomenklatur einiger Arten
624 der Gattung *Cystoseira* C. Ag. Nova Hedwigia, 26, 341–348.
625 Grant, G. T., Morris, E. R., Rees, D. A., Smith, P. J., & Thom, D. (1973). Biological
626 interactions between polysaccharides and divalent cations: the egg-box model. *FEBS*
627 *letters*, *32*(1), 195–198.
628 Hentati, F., Delattre, C., Ursu, A. V., Desbrières, J., Le Cerf, D., Gardarin, C.,
629 Abdelkafi, S., Michaud, P., & Pierre, G. (2018). Structural characterization and antioxidant
630 activity of water-soluble polysaccharides from the Tunisian brown seaweed *Cystoseira*
631 *compressa*. *Carbohydrate Polymers*, *198*, 589–600.

Hifney, A. F., Fawzy, M. A., Abdel-Gawad, K. M., & Gomaa, M. (2016). Industrial optimization of fucoidan extraction from *Sargassum* sp. and its potential antioxidant and emulsifying activities. *Food hydrocolloids*, 54, 77-88.

Katayama, S., Nishio, T., Iseya, Z., Kishimura, H., & Saeki, H. (2009). Effects of manufacturing factors on the viscosity of a polysaccharide solution extracted from Gagome *Kjellmaniella crassifolia*. *Fisheries Science*, *75*(2), 491.

Kechinski, C. P., Schumacher, A. B., Marczak, L. D., Tessaro, I. C., & Cardozo, N. S. (2011). Rheological behavior of blueberry (*Vaccinium ashei*) purees containing xanthan gum and fructose as ingredients. *Food hydrocolloids*, *25*(3), 299–306.

Keleşoğlu, S., Pettersen, B. H., & Sjöblom, J. (2012). Flow properties of water-in-North Sea heavy crude oil emulsions. *Journal of Petroleum Science and Engineering*, *100*, 14–23.

Khajouei, R. A., Keramat, J., Hamdami, N., Ursu, A. V., Delattre, C., Laroche, C., ... & Michaud, P. (2018). Extraction and characterization of an alginate from the Iranian brown seaweed Nizimuddinia zanardini. *International journal of biological macromolecules*, *118*, 1073-1081.

Lapasin, R., & Pricl, S. (1999). Rheology of Industrial Polysaccharides; Theory and Applications (5th ed., pp. 1–620). Maryland, U.S.A: Aspen Publication.

Liu, X., Qian, L., Shu, T., & Tong, Z. (2003). Rheology characterization of sol–gel transition in aqueous alginate solutions induced by calcium cations through in situ release. *Polymer*, *44*(2), 407–412.

Ma, J., Lin, Y., Chen, X., Zhao, B., & Zhang, J. (2014). Flow behavior, thixotropy and dynamical viscoelasticity of sodium alginate aqueous solutions. *Food Hydrocolloids*, *38*, 119–128.

Mancini, M., Moresi, M., & Sappino, F. (1996). Rheological behaviour of aqueous dispersions of algal sodium alginates. *Journal of Food Engineering*, *28*(3–4), 283–295.

Morris, E. R., Rees, D. A., & Thom, D. (1980). Characterization of alginate composition and block-structure by circular dichroism. *Carbohydrate Research*. 81(2), 305-314.

Norton I.T., Morris E.R., & Rees D.A. (1984). Lyotropic effects of simple anions on the conformation and interactions of kappa-carrageenan. *Carbohydrate Research*, *134(1)*, 89–101.

Oliveira, J. D., Silva, D. A., De Paula, R. C. M., Feitosa, J. P. A., & Paula, H. C. B. (2001). Composition and effect of salt on rheological and gelation properties of *Enterolobium contortisilliquum* gum exudate. *International Journal of Biological Macromolecules*, *29*(1), 35–44.

Palanisamy, S., Vinosha, M., Marudhupandi, T., Rajasekar, P., & Prabhu, N. M. (2017). Isolation of fucoidan from *Sargassum polycystum* brown algae: Structural characterization, in vitro antioxidant and anticancer activity. *International journal of biological macromolecules*, *102*, 405-412.

Plazinski, W. (2011). Molecular basis of calcium binding by polyguluronate chains. Revising the Egg-Box model. *Journal of Computational Chemistry*, *32*, 2988-2995.

Razavi, S. M. A., Cui, S. W., & Ding, H. (2016). Structural and physicochemical characteristics of a novel water-soluble gum from *Lallemantia royleana* seed. *International journal of biological macromolecules*, *83*, 142–151.

Razmkhah, S., Razavi, S. M. A., & Mohammadifar, M. A. (2017). Dilute solution, flow behavior, thixotropy and viscoelastic characterization of cress seed (*Lepidium sativum*) gum fractions. *Food Hydrocolloids*, *63*, 404–413.

680 Rhein-Knudsen, N., Ale, M.T., & Meyer, A.S. (2015). Seaweed hydrocolloid
681 production: an update on enzyme assisted extraction and modification technologies. *Marine*
682 *Drugs, 13*, 3340-3359.
683 Rioux, L. E., Turgeon, S. L., & Beaulieu, M. (2007). Rheological characterization of
684 polysaccharides extracted from brown seaweeds. *Journal of the Science of Food and*
685 *Agriculture*, *87*(9), 1630–1638.
686 Sabra, W., & Deckwer, W. D. (2005). Alginate-A polysaccharide of industrial interest
687 and diverse biological functions. Polysaccharides-structural diversity and functional
688 versatility, *2nd edn. Marcel Dekker, New York*, 515-533.
689 Sanjeewa, K. A., Kang, N., Ahn, G., Jee, Y., Kim, Y. T., & Jeon, Y. J. (2018).
690 Bioactive potentials of sulfated polysaccharides isolated from brown seaweed *Sargassum* spp
691 in related to human health applications: A review. *Food hydrocolloids*, 81, 200-208.
692 Seale, R., Morris, E. R., & Rees, D. A. (1982). Interactions of alginates with univalent
693 cations. *Carbohydrate Research*, *110*(1), 101–112.
694 Simas-Tosin, F. F., Barraza, R. R., Petkowicz, C. L. O., Silveira, J. L. M., Sassaki, G.
695 L., Santos, E. M. R., et al. (2010). Rheological and structural characteristics of peach tree gum
696 exudate. *Food Hydrocolloids*, *24*(5), 486–493.
697 Sosa-Herrera, M. G., Lozano-Esquivel, I. E., de León-Ramírez, Y. P., & Martínez-
698 Padilla, L. P. (2012). Effect of added calcium chloride on the physicochemical and
699 rheological properties of aqueous mixtures of sodium caseinate/sodium alginate and
700 respective oil-in-water emulsions. *Food hydrocolloids*, *29*(1), 175–184.
701 Vinogradov, G.V., Malkin, A. Y. (1980). Rheology of Polymers: Viscoelasticity and
702 Flow of Polymers. Moscow: Mir; New York: Springer-Verlag, 105–121.
703 Tako, M. (2003). Rheological characteristics of fucoidan isolated from commercially
704 cultured *Cladosiphon okamuranus*. *Botanica marina*, *46*(5), 461–465.

Tako, M., Yoza, E., & Tohma, S. (2000). Chemical characterization of acetyl fucoidan and alginate from commercially cultured *Cladosiphon okamuranus*. *Botanica Marina*, *43*(4), 393–398.

Xiao, Q., Tong, Q., & Lim, L. T. (2012). Pullulan-sodium alginate based edible films: Rheological properties of film forming solutions. *Carbohydrate Polymers*, *87*(2), 1689–1695.

Xu, X., Xue, C., Chang, Y., & Liu, G. (2017). Chain conformation, rheological and charge properties of fucoidan extracted from sea cucumber *Thelenota ananas*: A semi-flexible coil negative polyelectrolyte. Food chemistry, 237, 511-515.

Yang, X. H., & Zhu, W. L. (2007).Viscosity properties of sodium carboxymethyl-cellulose solutions. *Cellulose*, *14*(5), 409–417.

Yang, J., Chen, S., & Fang, Y. (2009).Viscosity study of interactions between sodium alginate and CTAB in dilute solutions at different pH values. *Carbohydrate Polymers*, *75*(2), 333–337.

Yu, L., Xue, C., Chang, Y., Hu, Y., Xu, X., Ge, L., & Liu, G. (2015). Structure and rheological characteristics of fucoidan from sea cucumber *Apostichopus japonicus*. *Food chemistry*, *180*, 71–76.

Figure captions

Fig. 1. (A) Flow behavior of aqueous CCSA solutions at different concentrations ranging from 0.25 to 5.0 % (w/v) at 25 °C. *Continuous solid line is obtained using the Newtonian data with* $\dot{\gamma}_c$, *the critical shear rate.* **(B)** Influence of salts (0.5 M NaCl and 0.5 M KCl) on the apparent viscosity of CCSA solutions ranging from 3.0 to 5.0 % (w/v) at 25 °C.

Fig. 2. (A) Steady-shear flow curves for aqueous CCSA solutions of 5.0 % (w/v) at different temperatures ranging from 20 to 60 °C. **(B)** Dependence of viscosity on temperatures (20-45 °C) for 5.0 % (w/v) CCSA solutions at shear rates ranging from 1 to 1000 s^{-1}. *Solid lines representing the fitted curves based on the Arrhenius-Frenkel-Eyring relationship*.

Fig. 3. Storage modulus (*G′*), loss modulus (*G″*) *vs*. angular frequency ($rad.s^{-1}$) for solutions of different concentration of CCSA at 25 °C in water **(A)** or in salts (0.5 M KCl and 0.5 M NaCl) **(B)**.

Fig. 4. Influence of divalent salt $CaCl_2$ at 25 °C on **(A)** flow apparent viscosity and **(B)** storage (*G′*) and loss (*G″*) moduli of aqueous solution of 2.0 % (w/v) CCSA.

Fig. 5. (A) Shear time dependence of CCSA flow curves at 25 °C. Shear stress *vs*. shear rate for different concentrations (3.0-5.0 %, w/v) of CCSA in water. **(B)** Critical overlap (C*) concentration obtained from the log-log plot of the specific viscosity (η_{sp}) versus the concentration of CCSA in water at 25 °C.

Fig. 6. (A) Steady-shear flow behavior curves of CCF solutions from 0.25 to 2.0 % (w/v) in water at 25 C. **(B)** Effect of monovalent salts concentrations (KCl and NaCl at 0.1-0.5 M) on the viscosity of CCSA solutions of 2.0 % (w/v) at 25 °C. **(C)** Flow curves as a function of temperature in the range of 20-60 °C for 1.0 % and 2.0 % (w/v) CCF solutions.

Fig. 7. (A) Dynamical oscillatory frequency sweep test curves of aqueous CCF solutions in concentration of 1.0 % and 2.0 % (w/v) at 25 °C. **(B)** Influence of NaCl and KCl (0.5 M) monovalent salts on storage modulus (*G′*) and loss modulus (*G″*) for 2.0% (w/v) CCF solution at 25 °C.

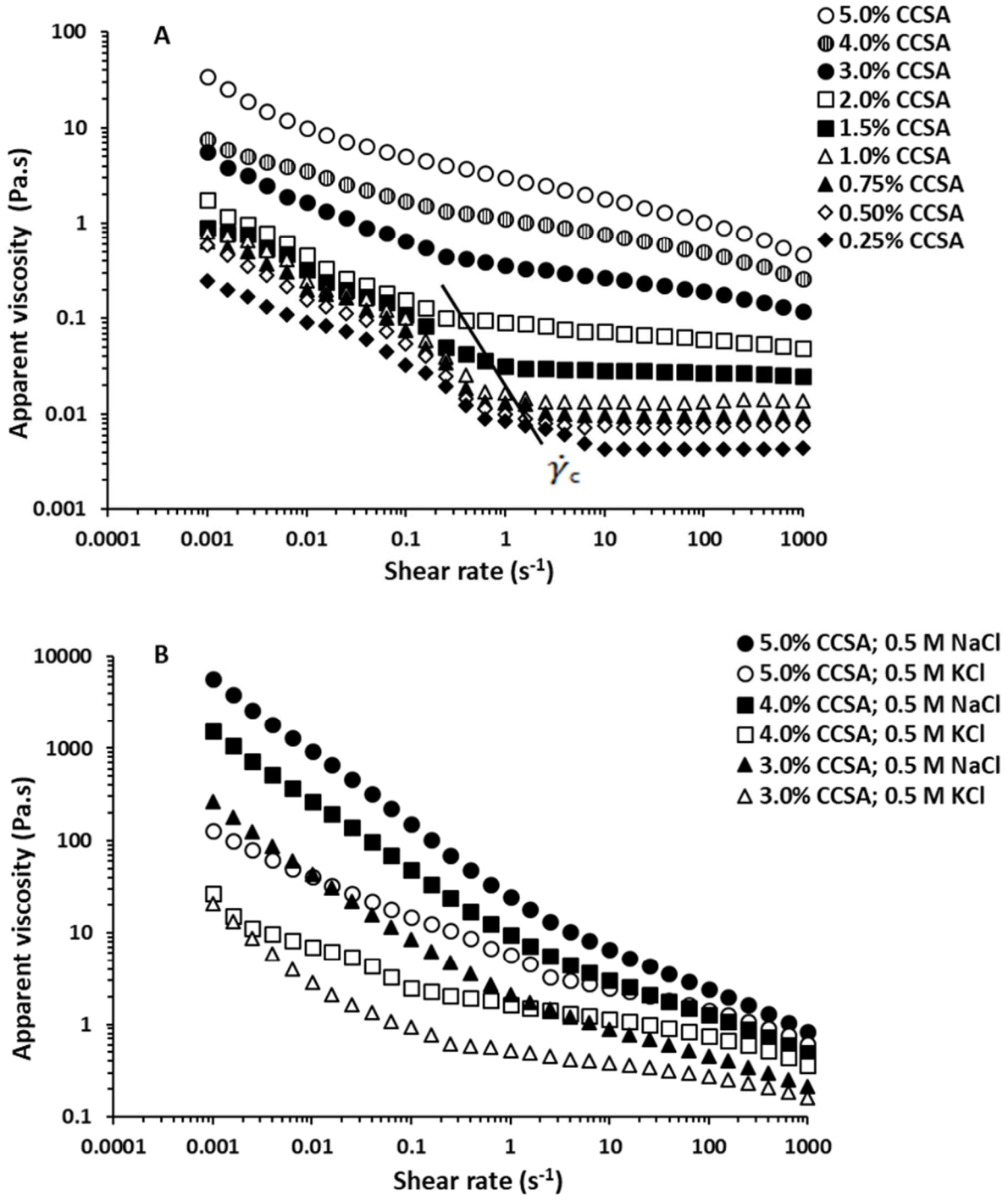
A
5.0% CCSA
4.0% CCSA
3.0% CCSA
2.0% CCSA
1.5% CCSA
1.0% CCSA
0.75% CCSA
0.50% CCSA
0.25% CCSA
Apparent viscosity (Pa.s)
Shear rate (s-1)
100
10
1
0.1
0.01
0.001
0.0001
0.001
0.01
0.1
1
10
100
1000
$\dot{\gamma}_c$
B
5.0% CCSA; 0.5 M NaCl
5.0% CCSA; 0.5 M KCl
4.0% CCSA; 0.5 M NaCl
4.0% CCSA; 0.5 M KCl
3.0% CCSA; 0.5 M NaCl
3.0% CCSA; 0.5 M KCl
Apparent viscosity (Pa.s)
Shear rate (s-1)
10000
1000
100
10
1
0.1
0.0001
0.001
0.01
0.1
1
10
100
1000

Figure 1.

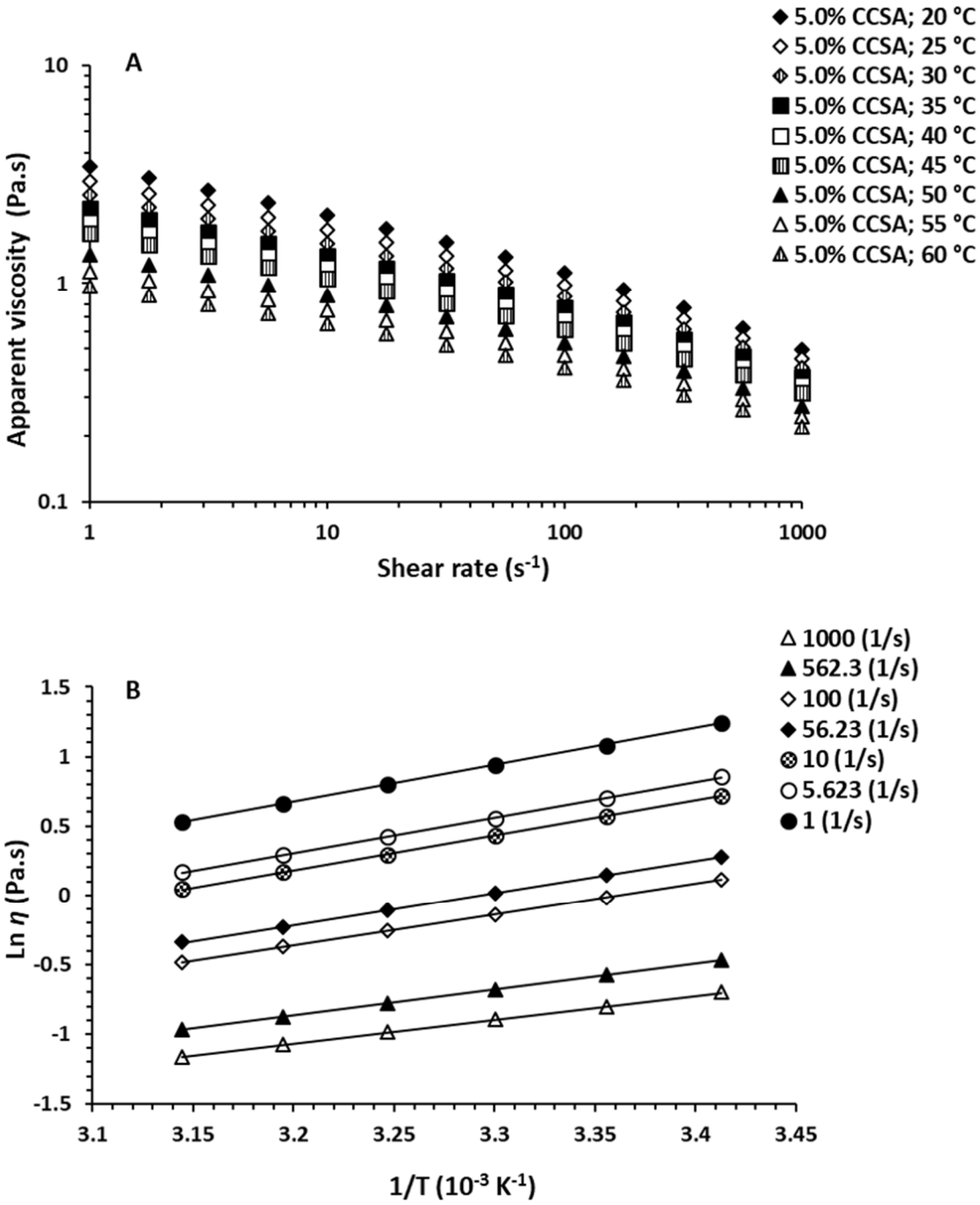
A
Apparent viscosity (Pa.s)
10
1
0.1
1
10
100
1000
Shear rate (s-1)
5.0% CCSA; 20 °C
5.0% CCSA; 25 °C
5.0% CCSA; 30 °C
5.0% CCSA; 35 °C
5.0% CCSA; 40 °C
5.0% CCSA; 45 °C
5.0% CCSA; 50 °C
5.0% CCSA; 55 °C
5.0% CCSA; 60 °C
B
Ln η (Pa.s)
1.5
1
0.5
0
-0.5
-1
-1.5
3.1
3.15
3.2
3.25
3.3
3.35
3.4
3.45
1/T (10-3 K-1)
1000 (1/s)
562.3 (1/s)
100 (1/s)
56.23 (1/s)
10 (1/s)
5.623 (1/s)
1 (1/s)

Figure 2.

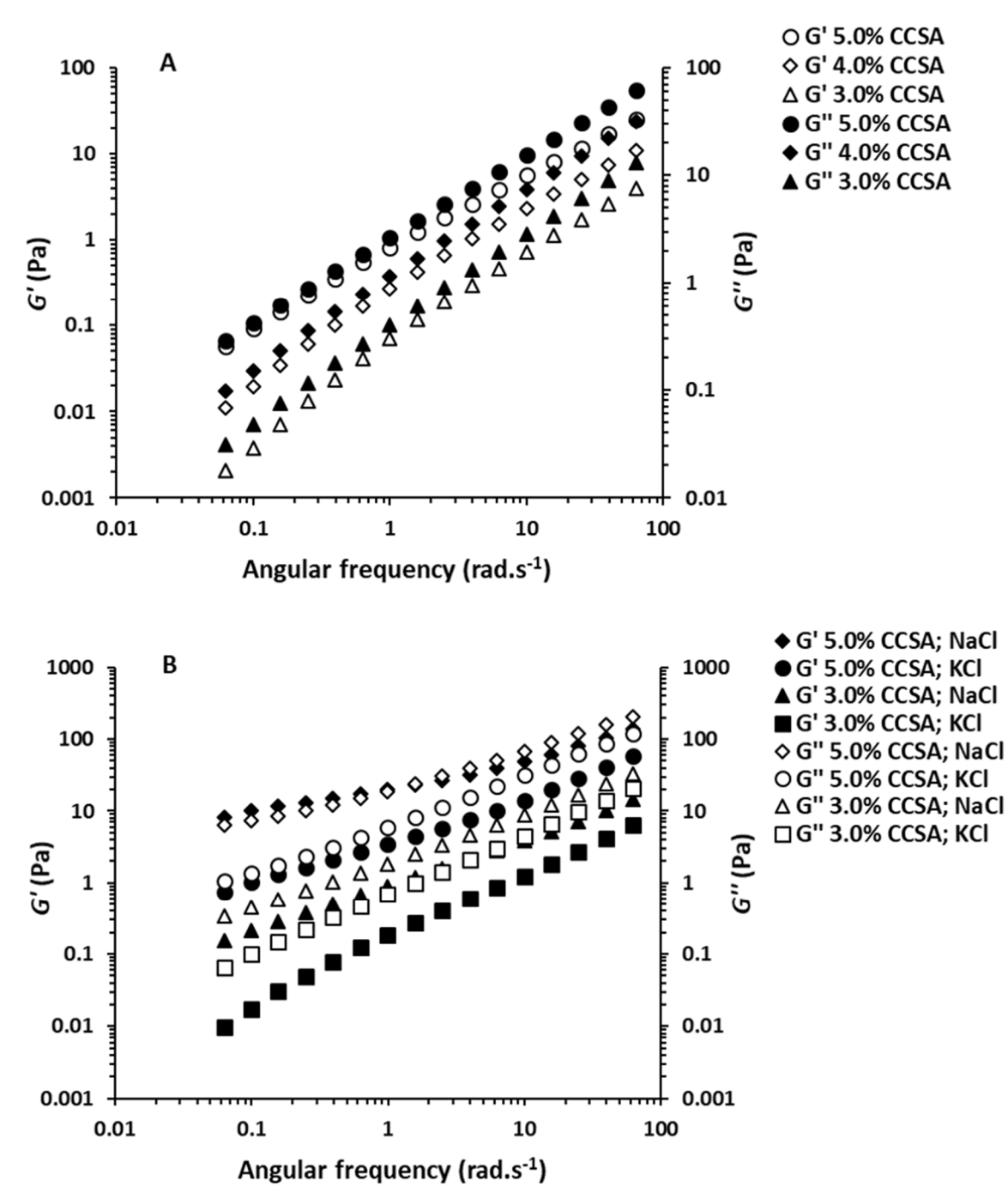
A
G' 5.0% CCSA
G' 4.0% CCSA
G' 3.0% CCSA
G'' 5.0% CCSA
G'' 4.0% CCSA
G'' 3.0% CCSA
G' (Pa)
G'' (Pa)
Angular frequency (rad.s-1)
B
G' 5.0% CCSA; NaCl
G' 5.0% CCSA; KCl
G' 3.0% CCSA; NaCl
G' 3.0% CCSA; KCl
G'' 5.0% CCSA; NaCl
G'' 5.0% CCSA; KCl
G'' 3.0% CCSA; NaCl
G'' 3.0% CCSA; KCl
G' (Pa)
G'' (Pa)
Angular frequency (rad.s-1)

Figure 3.

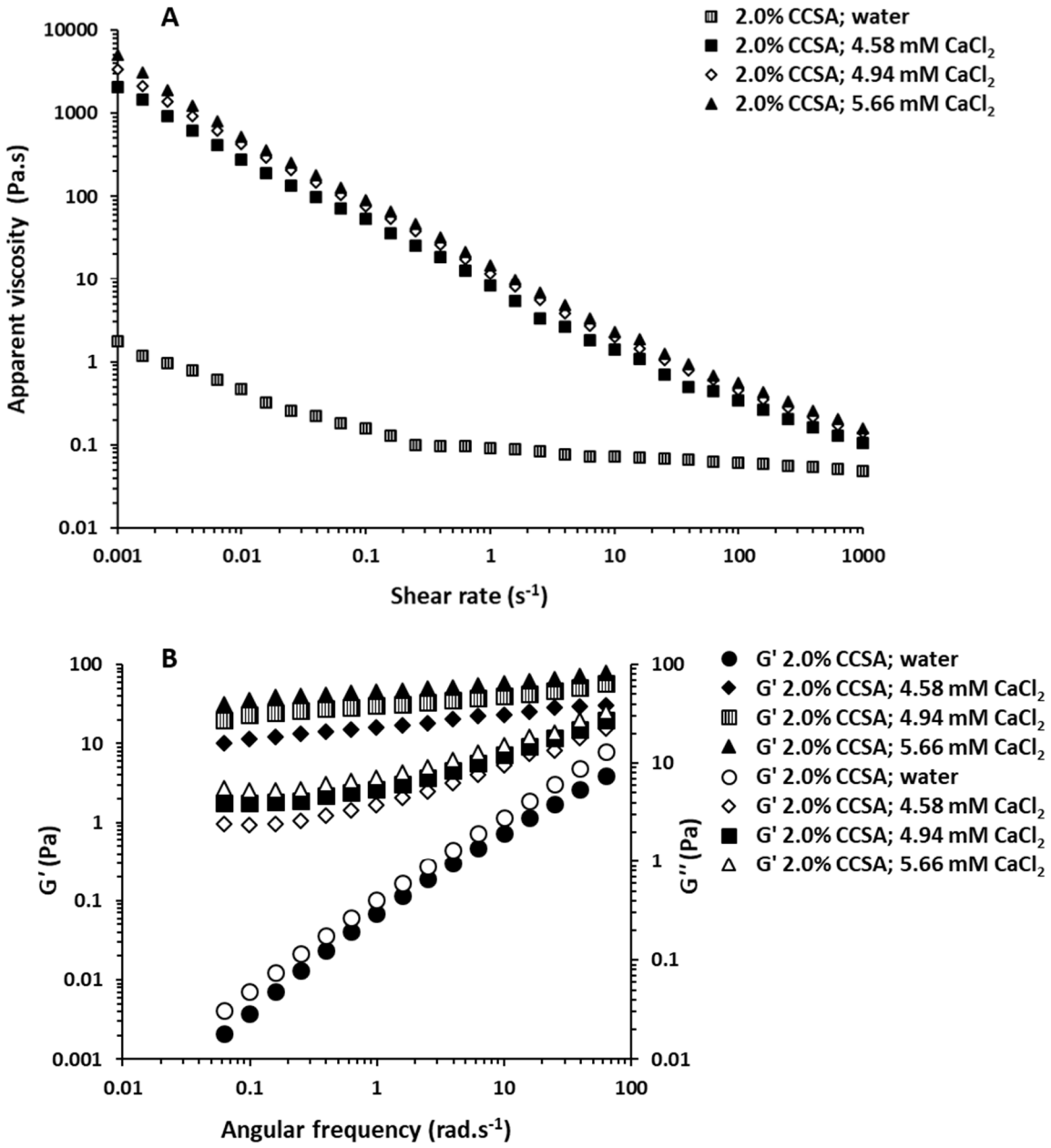
A
Apparent viscosity (Pa.s)
Shear rate (s-1)
2.0% CCSA; water
2.0% CCSA; 4.58 mM CaCl2
2.0% CCSA; 4.94 mM CaCl2
2.0% CCSA; 5.66 mM CaCl2
B
G′ (Pa)
G′′ (Pa)
Angular frequency (rad.s-1)
G' 2.0% CCSA; water
G' 2.0% CCSA; 4.58 mM CaCl2
G' 2.0% CCSA; 4.94 mM CaCl2
G' 2.0% CCSA; 5.66 mM CaCl2
G' 2.0% CCSA; water
G' 2.0% CCSA; 4.58 mM CaCl2
G' 2.0% CCSA; 4.94 mM CaCl2
G' 2.0% CCSA; 5.66 mM CaCl2

Figure 4.

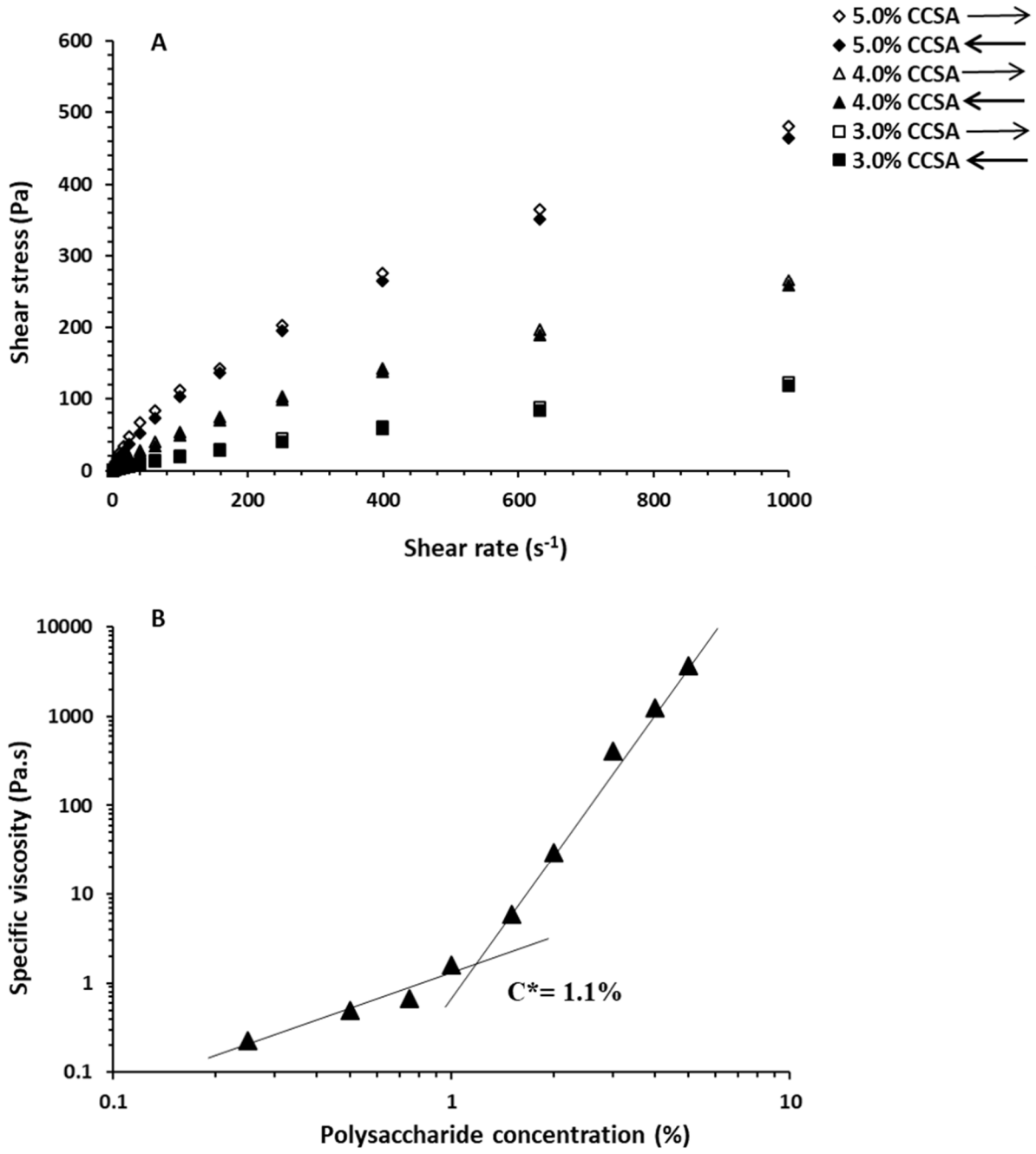
A
5.0% CCSA
5.0% CCSA
4.0% CCSA
4.0% CCSA
3.0% CCSA
3.0% CCSA
Shear stress (Pa)
Shear rate (s-1)
B
Specific viscosity (Pa.s)
Polysaccharide concentration (%)
C*= 1.1%

Figure 5.

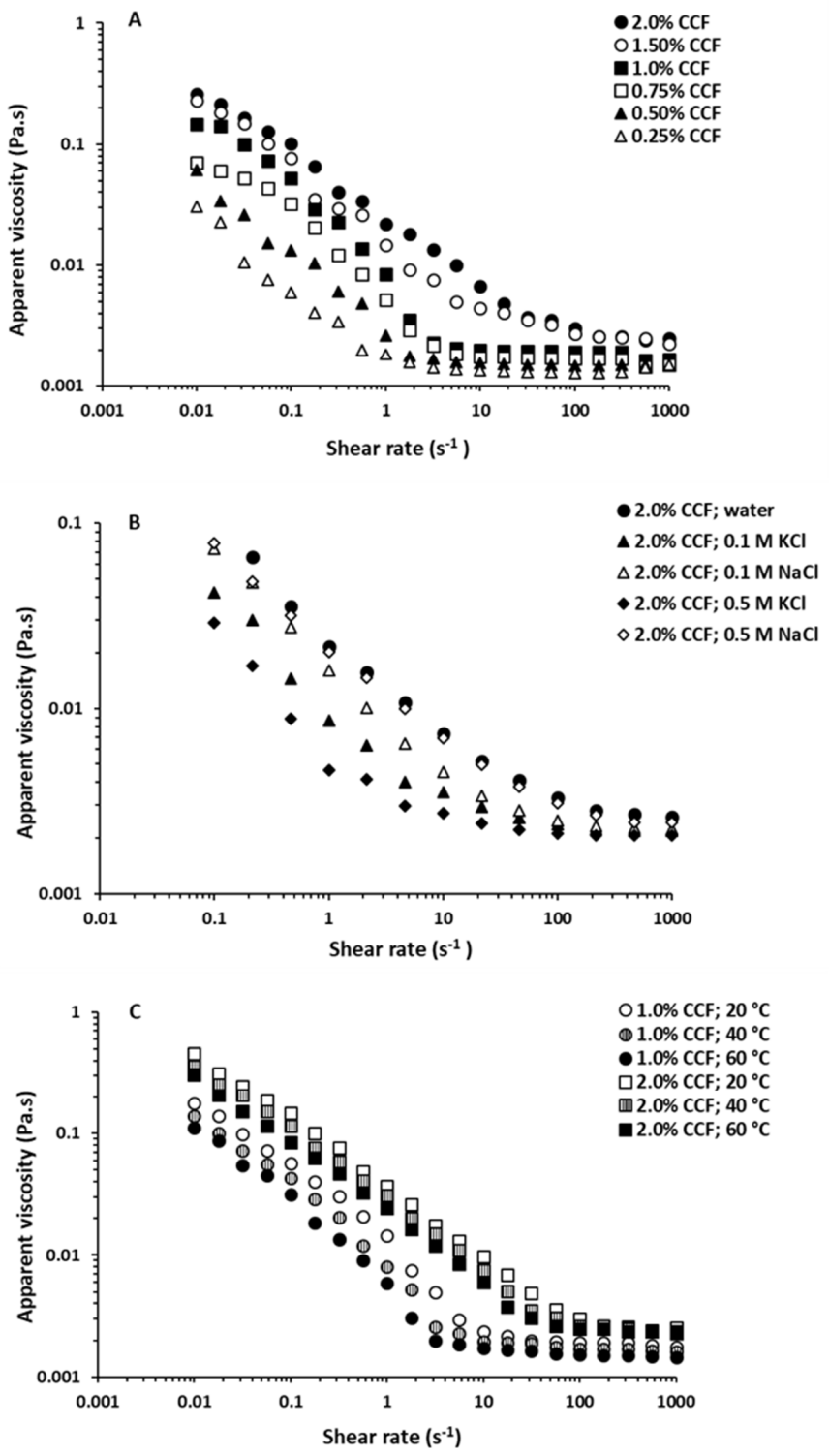
A
2.0% CCF
1.50% CCF
1.0% CCF
0.75% CCF
0.50% CCF
0.25% CCF
Apparent viscosity (Pa.s)
Shear rate (s-1)
B
2.0% CCF; water
2.0% CCF; 0.1 M KCl
2.0% CCF; 0.1 M NaCl
2.0% CCF; 0.5 M KCl
2.0% CCF; 0.5 M NaCl
Apparent viscosity (Pa.s)
Shear rate (s-1)
C
1.0% CCF; 20 °C
1.0% CCF; 40 °C
1.0% CCF; 60 °C
2.0% CCF; 20 °C
2.0% CCF; 40 °C
2.0% CCF; 60 °C
Apparent viscosity (Pa.s)
Shear rate (s-1)

Figure 6.

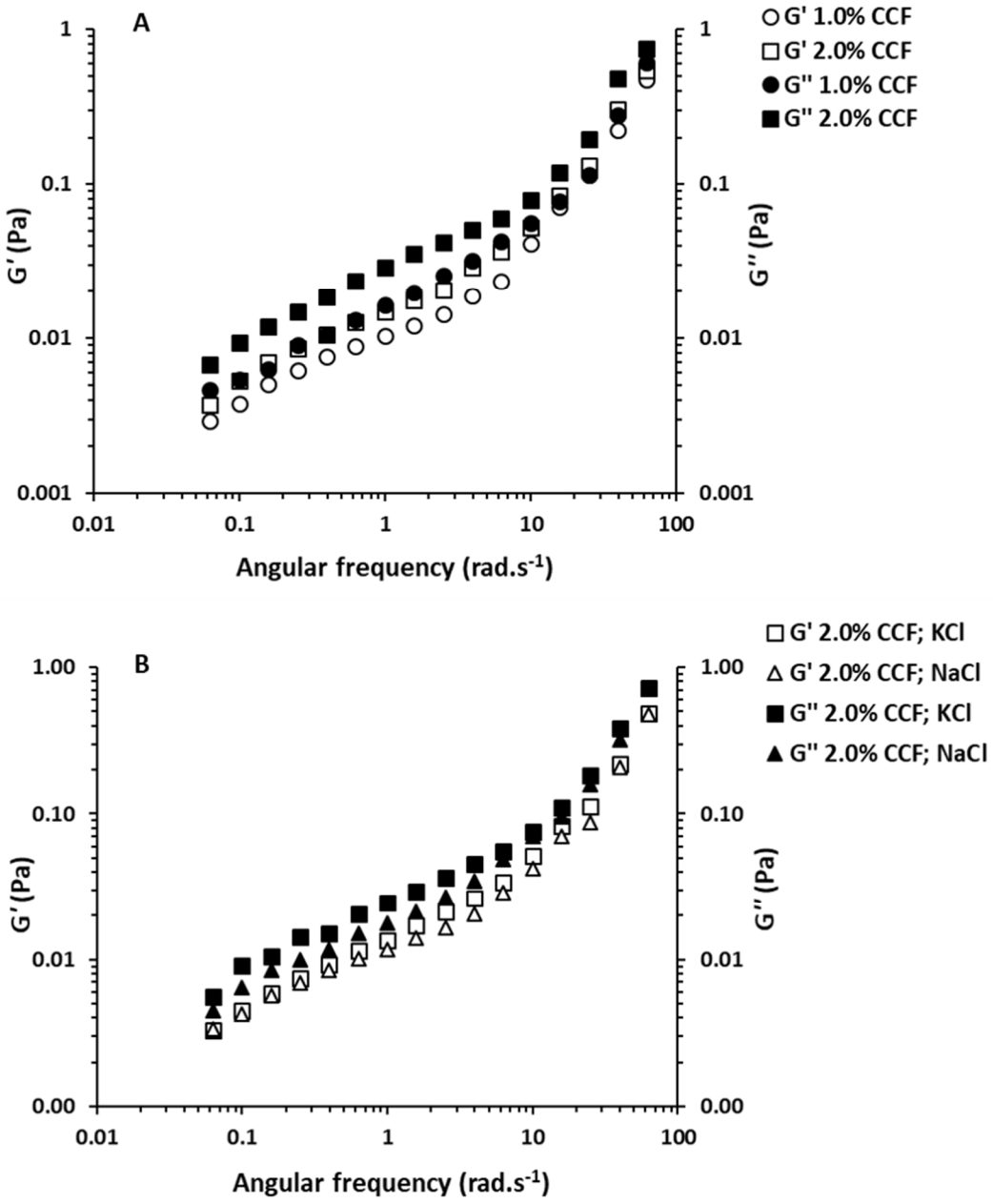
A
G' 1.0% CCF
G' 2.0% CCF
G'' 1.0% CCF
G'' 2.0% CCF
G′ (Pa)
G′′ (Pa)
Angular frequency (rad.s-1)
B
G' 2.0% CCF; KCl
G' 2.0% CCF; NaCl
G'' 2.0% CCF; KCl
G'' 2.0% CCF; NaCl
G′ (Pa)
G′′ (Pa)
Angular frequency (rad.s-1)

Figure 7.

List of Tables

Table 1.

CCSA (%, w/v)	Ostwald-de Waele model fitting parameters		
	n	***k***	R^2
2.0	0.772 ± 0.015	0.141 ± 0.004	0.983
3.0	0.753 ± 0.007	0.499 ± 0.075	0.992
4.0	0.781 ± 0.009	1.224 ± 0.106	0.998
5.0	0.730 ± 0.005	3.226 ± 0.125	0.997
CCF (%, w/v)	**Ostwald-de Waele model fitting parameters**		
	n	***k***	R^2
0.25	1.093 ± 0.022	0.004 ± 0.001	0.963
0.50	0.987 ± 0.013	0.007 ± 0.003	0.971
0.75	0.949 ± 0.004	0.012 ± 0.008	0.975
1.0	0.929 ± 0.018	0.018 ± 0.005	0.984
1.5	0.895 ± 0.005	0.047 ± 0.003	0.971
2.0	0.868 ± 0.010	0.077 ± 0.001	0.986

Table 2.

CCSA	**Parameters**	**Shear rate (s^{-1})**						
(%, w/v)		1	5.623	10	56.23	100	562.3	1000
3.0	E_a (Kcal.mol^{-1})	5.473	5.017	4.931	4.674	4.576	4.131	3.919
	R^2	0.998	0.998	0.998	0.998	0.998	0.999	0.999
4.0	E_a (Kcal.mol^{-1})	5.488	5.147	5.064	4.709	4.547	3.942	3.692
	R^2	0.999	0.999	0.999	0.999	0.999	0.999	0.999
5.0	E_a (Kcal.mol^{-1})	5.248	5.061	4.972	4.577	4.403	3.696	3.399
	R^2	0.999	0.999	0.999	0.999	0.999	1.000	1.000

Table 3

CCSA (%, w/v)	NaCl (mol.L^{-1})	KCl (mol.L^{-1})	*n*	*k*	R^2
3.0	0.0	0.0	0.753 ± 0.007	0.499 ± 0.075	0.992
	0.0	0.1	0.721 ± 0.033	0.686 ± 0.093	0.986
	0.1	0.0	0.664 ± 0.029	1.022 ± 0.154	0.983
	0.0	0.5	0.711 ± 0.042	0.801 ± 0.141	0.976
	0.5	0.0	0.499 ± 0.037	3.683 ± 0.568	0.963
4.0	0.0	0.0	0.781 ± 0.009	1.224 ± 0.106	0.998
	0.0	0.1	0.761 ± 0.018	1.504 ± 0.245	0.999
	0.1	0.0	0.602 ± 0.036	3.349 ± 0.509	0.975
	0.0	0.5	0.741 ± 0.022	2.072 ± 0.382	0.994
	0.5	0.0	0.418 ± 0.034	15.376 ± 2.163	0.961
5.0	0.0	0.0	0.730 ± 0.005	3.226 ± 0.125	0.997
	0.0	0.1	0.675 ± 0.011	4.985 ± 0.565	0.995
	0.1	0.0	0.542 ± 0.008	8.955 ± 0.263	0.999
	0.0	0.5	0.626 ± 0.017	6.915 ± 0.97	0.995
	0.5	0.0	0.356 ± 0.032	39.706 ± 5.176	0.948
CCF (%, w/v)					
2.0	0.0	0.0	0.606 ± 0.025	0.026 ± 0.004	0.975
	0.0	0.1	0.683 ± 0.018	0.011 ± 0.00	0.968
	0.1	0.0	0.607 ± 0.009	0.018 ± 0.003	0.965
	0.0	0.5	0.742 ± 0.013	0.007 ± 0.001	0.979
	0.5	0.0	0.608 ± 0.008	0.002 ± 0.00	0.988

Table 4.

CCSA (%, w/v)	NaCl (mol.L^{-1})	KCl (mol.L^{-1})	Power-law model fitting parameters					
			n'	n''	k'	k''	R'^2	R''^2
3.0	0.0	0.0	1.083 ± 0.013	0.871 ± 0.011	0.058 ± 0.001	0.381 ± 0.014	0.995	0.999
	0.5	0.0	0.645 ± 0.027	0.662 ± 0.008	0.899 ± 0.013	1.941 ± 0.178	0.999	0.998
	0.0	0.5	0.905 ± 0.012	0.827 ± 0.024	0.161 ± 0.005	0.675 ± 0.019	0.996	0.999
4.0	0.0	0.0	0.989 ± 0.006	0.829 ± 0.002	0.229 ± 0.009	1.088 ± 0.048	0.995	0.999
	0.5	0.0	0.479 ± 0.011	0.586 ± 0.018	5.629 ± 0.108	7.272 ± 0.309	0.989	0.994
	0.0	0.5	0.833 ± 0.009	0.805 ± 0.010	0.547 ± 0.033	1.878 ± 0.036	0.998	0.999
5.0	0.0	0.0	0.871 ± 0.010	0.774 ± 0.003	0.753 ± 0.011	2.569 ± 0.0151	0.998	0.999
	0.5	0.0	0.389 ± 0.016	0.515 ± 0.016	21.704 ± 1.383	21.279 ± 0.175	0.981	0.990
	0.0	0.5	0.614 ± 0.007	0.700 ± 0.012	3.736 ± 0.576	6.320 ± 0.269	0.994	0.998
CCF (%, w/v)								
2.0	0.0	0.0	0.636 ± 0.015	0.601 ± 0.017	0.018 ± 0.003	0.031 ± 0.005	0.948	0.943
	0.0	0.5	0.694 ± 0.008	0.659 ± 0.021	0.014 ± 0.001	0.024 ± 0.003	0.963	0.946
	0.5	0.0	0.693 ± 0.011	0.638 ± 0.009	0.011 ± 0.001	0.021 ± 0.00	0.938	0.944

Table 5.

CCSA (%, w/v)	$CaCl_2$ (mmol.L^{-1})	Power-law model fitting parameters					
		n'	n''	k'	k''	R'^2	R''^2
2.0	0.00	1.457 ± 0.145	0.996 ± 0.010	0.001 ± 0.00	0.077 ± 0.013	0.985	1.000
	4.58	0.143 ± 0.008	0.345 ± 0.005	21.145 ± 0.511	4.461 ± 0.213	0.979	0.961
	4.94	0.132 ± 0.001	0.344 ± 0.003	30.399 ± 0.415	5.759 ± 0.619	0.983	0.964
	5.30	0.119 ± 0.005	0.309 ± 0.007	32.114 ± 0.653	7.223 ± 0.414	0.963	0.960
	5.66	0.115 ± 0.004	0.250 ± 0.003	45.709 ± 1.091	9.589 ± 0.683	0.984	0.928

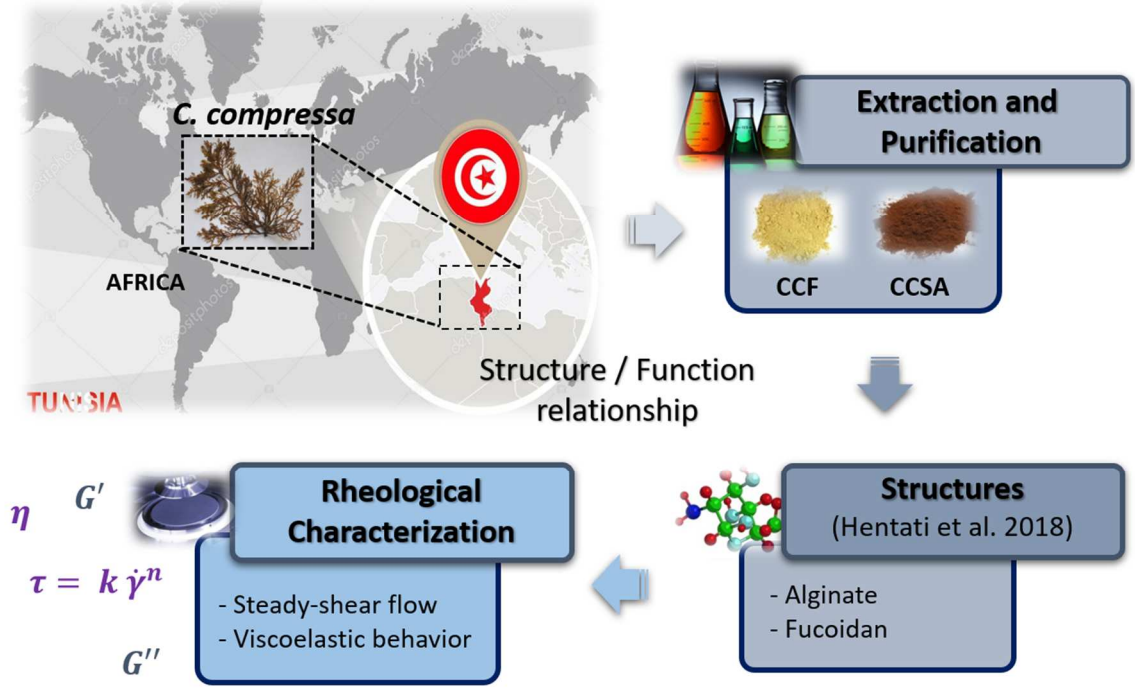

Graphical abstract: Investigation of flow behavior and dynamical viscoelasticity of water-soluble polysaccharides from *C. compressa* (Tunisian brown seaweed).